condensed matter

MDPI

Article

Challenging X-ray Fluorescence Applications for Environmental Studies at XLab Frascati

Giorgio Cappuccio [1], Giannantonio Cibin [2], Sultan B. Dabagov [1,3,4], Alfredo Di Filippo [5], Gianluca Piovesan [5], Dariush Hampai [1]*, Valter Maggi [6,7] and Augusto Marcelli [1,8]

1 INFN-LNF, XLab Frascati, Via E. Fermi 40, I-00044 Rome, Italy; cappuccio.giorgio@gmail.com (G.C.); sultan.dabagov@lnf.infn.it (S.B.D.); augusto.marcelli@lnf.infn.it (A.M.)
2 Diamond Light Source Ltd., Harwell Science and Innovation Campus, Didcot OX11 0DE, UK; giannantonio.cibin@diamond.ac.uk
3 RAS P.N. Lebedev Physical Institute, Moscow 119991, Russia
4 National Research Nuclear University MEPhI, Moscow 115409, Russia
5 Dendrology Lab, Department of Agriculture and Forestry Science (DAFNE), University Tuscia, 01100 Viterbo, Italy; difilippo@unitus.it (A.D.F.); piovesan@unitus.it (G.P.)
6 Earth and Environmental Sciences Department, University of Milano-Bicocca, 20126 Milano, Italy; valter.maggi@unimib.it
7 INFN Section of Milano-Bicocca, 20126 Milano, Italy
8 RICMASS, Rome International Center for Materials Science Superstripes, Via dei Sabelli 119A, 00185 Roma, Italy
* Correspondence: dariush.hampai@lnf.infn.it; Tel.: +39-06-9403-5248

Received: 31 July 2018; Accepted: 12 October 2018; Published: 18 October 2018

Abstract: In this work, we will report applications of the total external X-ray fluorescence (TXRF) station, a prototype assembled at the XLab Frascati laboratory (XlabF) at the INFN National Laboratories of Frascati (INFN LNF). XlabF has been established as a facility to study, design and develop X-ray optics, in particular, polycapillary lenses, as well as to perform X-ray experiments for both elemental analysis and tomography. The combination of low-power conventional sources and policapillary optics allows assembling a prototype that can provide a quasi-parallel intense beam for detailed X-ray spectroscopic analysis of extremely low concentrated samples, down to ng/g. We present elemental analysis results of elements contained in tree rings and of dust stored in deep ice cores. In addition to performing challenging environmental research studies, other experiments aim to characterize novel optics and to evaluate original experimental schemes for X-ray diffraction (XRD), X-ray fluorescence (XRF and TXRF) and X-ray imaging.

Keywords: TXRF; polycapillary optics; low concentration elemental analysis

1. Introduction

Due to the large penetration depth of X-rays, a variety of analytical techniques, such as X-ray fluorescence (XRF), X-ray diffraction (XRD) and 3D tomography may be used to study the inner sample structure without any destructive preparation [1–3]. Among these techniques, XRF is a method widely used in many different fields to characterize qualitatively and quantitatively the elemental composition of the samples in a non-destructive way (for example, [4,5] and related).

The continuous development of large facilities, such as Synchrotron Radiation (SR) and Free Electron Laser (FEL), together with the significant improvements in X-ray optics greatly expanded the application X-ray techniques for elemental analysis, spectroscopy and imaging studies. In particular, XRF is now commonly utilized as an *ab initio* technique both for qualitative and quantitative analysis, to investigate the composition of a sample down to very low concentrations [6,7]. However, the growth

of applications and of users makes the number of available SR sources insufficient to accommodate the requests and many beamlines devoted to X-ray studies are fully packed. As a consequence SR facilities are not available for routine analysis and for many studies the only alternative approach is the use of powerful X-ray microfocus sources coupled to polycapillary optics (PolyCO) [8]. Indeed, the combination of a polycapillary lens with a fine-focus X-ray tube makes it possible to achieve a focusing spot with diameters less than 50 μm. Moreover, it can provide the intensity radiation flux necessary to perform challenging elemental analysis [9]. One of the most attractive applications of such configuration is the confocal geometry with two conjugated X-ray polycapillary lenses [2,9,10]. This peculiar geometry allows one to control the depth of the XRF signal leading to the possibility of depth profile analysis. Due to the high-intensity irradiation on a limited sample area, both non-destructive μXRF analysis and 2D/3D elemental mapping are now possible. Moreover, in the total external reflection X-ray fluorescence regime (TXRF) [11], the decreased detection limits and the lower noises are directly correlated to the lower measurable concentration. To apply this special technique in a simpler way, an incident parallel beam is required. This can be achieved by replacing the primary polycapillary full-lens with a semi-lens, which transforms the divergent source beam into a quasi-parallel one. As shown below, this technique enables excellent results, sometime comparable with those obtained at SR facilities, even for samples with low elemental concentrations [6,7,12].

Among the most interesting applications of this technique is elemental analysis for environmental research. This is a highly demanding application not only in term of recognition of low Z (Na, Al, Mg, K, Ca, etc.) and high Z elements (Fe, Mn, As, Hg, etc.) but also for the large number of samples investigated, sometimes up to hundreds. In the latter case, the time request (several shifts) is hard to fulfill at synchrotron radiation facilities and sometimes the process requires more than one beamline. Moreover, the number of available SR beamlines suitable for these studies is relatively limited and many of them are oversubscribed. Consequently, the use of SR facilities for proposals highly demanding in time and for routine analysis is not straightforward and environmental and climatic studies are not easily performed at these large facilities. As an alternative, a promising approach is the use of X-ray microfocus sources enhanced by means of polycapillary optics [8]. In this contribution, we will show in Section 3.1 some representative examples of tree rings [13] and deep ice cores [14–16] analyzed with an experimental layout based on a combination of polycapillary lens and fine-focus X-ray tubes that can provide high-intensity radiation fluxes. Operating in a total external reflection regime (TXRF), the reduction of noise allows for the improvement of the detection limits, which is a fundamental aspect to be considered in the analysis of a sample with low elemental concentrations. To apply this special technique in a simpler way, an incident parallel beam is required. This can be achieved by replacing the primary polycapillary full-lens with a semi-lens, which converts the divergent source beam into a quasi-parallel one.

The analysis of tree rings is a powerful historical ecology tool for identifying and quantifying important relationships between tree growth and climatic events [17]. Similar to tree rings, deep ice cores taken from polar and continental glaciers are other fundamental natural archives of paleoclimatic information, which can provide unaltered records of environmental and climatic changes at different time scales dating back to several hundred thousand years. The mineralogical composition as well as the size distribution of particles are mainly related to the selection occurring in the atmosphere during dust transport. Nowadays, aeolian mineral dust in thin sections of the Antarctic deep ice cores is actively studied in order to assess the climate changes in the Late Quaternary in the Southern Hemisphere [14,15].

2. XLab Frascati

Since early 2000, a great effort has been devoted at the LNF-INFN to make available the XLab Frascati (XlabF) [18], an optical laboratory dedicated to the study of X-ray optics, in particular, polycapillary lenses and other exotic optical elements. Presently, two facility stations (RXR and XENA, Table 1) are available to users [18], optimizing and matching different analytical techniques.

In particular, the XENA (X-ray experimental station for non-destructive analysis) station, operative since 2004, is equipped with three X-ray Oxford Apogee tubes (W, Mo and Cu anodes), a set of mechanical components and motors for lens alignment and scanning and an optical table with different geometrical layouts. At first it was used for all X-ray analysis. Now the facility is dedicated to imaging, tomography and characterization of X-ray devices, such as novel sources [19], optics [20], diffractive crystals [21], vibrating systems [22], fast processes [23], high-resolution imaging [24] and new detectors [25].

Table 1. XLab frascati facilities.

	XENA	**RXR**
Station	X-ray Elemental station for Non-destructive Analysis	Rainbow X-ray
Analysis	(1) High Resolution Imaging (2) μCT (3) X-ray Optics Characterization (4) Detector Characterization (5) Novel Sources	(1) μXRF (2D and 3D mapping) (2) TXRF
Resolution	(1) <1 μm [24] (2) $<17 \times 17 \times 17$ μm^3 [23]	(1) $\sim 80 \times 80$ μm^2 [9] $\sim 80 \times 80 \times 80$ μm^3 [9] (2) 25 ± 1.25 ng/g concentrations [20]

The RXR (Rainbow X-ray) station is an apparatus optimized for 2D/3D XRF micro-imaging and TXRF [9,10]. It is equipped with two detectors characterized by different energy efficiency, covering the wide spectral range from 800 eV to 25 keV. The station works in the confocal geometry, i.e., the source is coupled to a full-lens and both detectors have dedicated half-lenses to match the emission. Samples can be investigated in air or inside a dedicated vacuum chamber that may extend the working capabilities down to the low energy.

A TXRF prototype spectrometer using a polycapillary semi-lens (the layout and its parameters are respectively in Figure 1 and in Table 2) has also been designed and assembled at XlabF. The optics are characterized according to the protocol developed in our lab and described in [20]. The optimum input focal distance of the lens used has been determined by performing a spatial scan of the lens with respect to the X-ray source, while the transmitted radiation has been monitored with a scintillator. The low divergence of this instrument allows one to detect the radiation peak intensity at ∼40 cm from the lens exit.

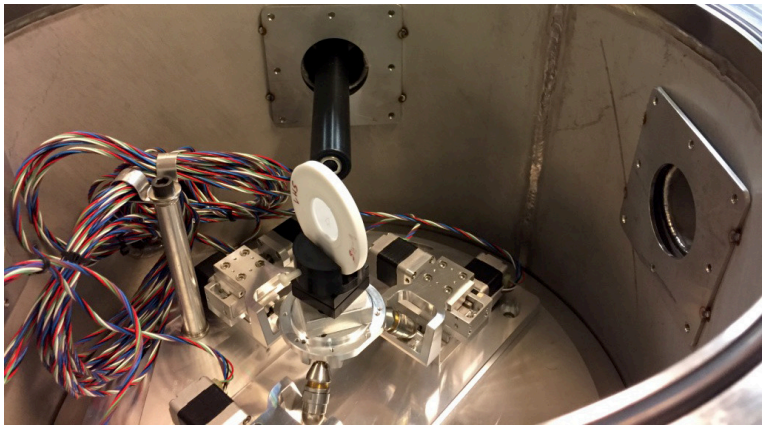

Figure 1. Total external reflection X-ray fluorescence (TXRF) prototype of the X-ray spectrometer. The vacuum chamber works down 10^{-5} hPa, while the positioning system allows independent translations and rotations along six axes $xyz\theta\phi\chi$.

Table 2. Parameters of the TXRF experimental layout.

2 X-ray Tubes [26]	Oxford Apogee 5000 - MoKα - W bremsstrahlung inelastic radiation source spot <50 µm power: 50 W
Silicon Drift Detector [27]	active area: 30 mm^2 with AP3.7 window
CCD Camera (FDI 1:1.61) [28]	pixel resolution: 10.4 × 10.4 µm^2
Polycapillary semi-lens [20]	Focal Distance: 59 mm transmission ∼60% residual divergence: 1.4 mrad

In this layout, for measurements at low energies, the sample can be positioned in a vacuum chamber working down to 10^{-5} hPa. Inside the vacuum chamber, the positioning is performed by means of a "hexapode micro-positioner" [29]. Such a device allows the translations along six axes $xyz\theta\phi\chi$ with a resolution of 0.5 µm and 19 µrad, Figure 1.

3. TXRF Results

The main experimental parameters for a TXRF prototype are the mass resolution and the minimum detection limit achievable in low concentrated samples. To determine these figures we analyzed standards for XFR, TXRF (Figure 2) by Axo [30] (Table on Supplementary Materials) and by NIST [9].

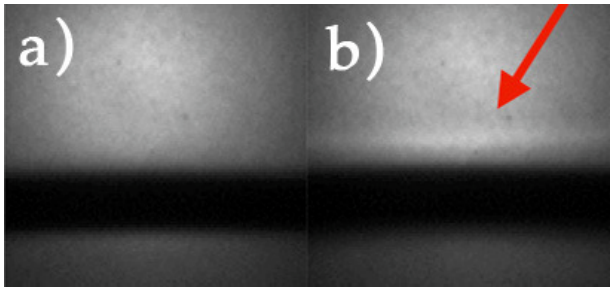

Figure 2. CCD images of the incident beam on AXO sample coated on a silicon wafer): (**a**) out of the total reflection regime and (**b**) in the TXRF regime. The reflected beam is indicated by a red arrow. The black area is due to absorption by the sample.

In Figure 3, the TXRF spectra of two different sources are compared. In this way it is possible to resolve both the elastic (MoKα) and anelastic radiation (W Bremsstrahlung) from the anode. The AXO sample spectrum was provided by the company and collected using a synchrotron radiation source [30].

Neglecting the variation in the spectra of the elastic and the inelastic peaks due to the different sources, the results are in good agreement with the AXO data. Moreover, the energy resolution is improved with respect to the AXO spectrum (e.g., in Figure 3 together with the Pd–L and La–L lines and the splitting of the FeKα and FeKβ).

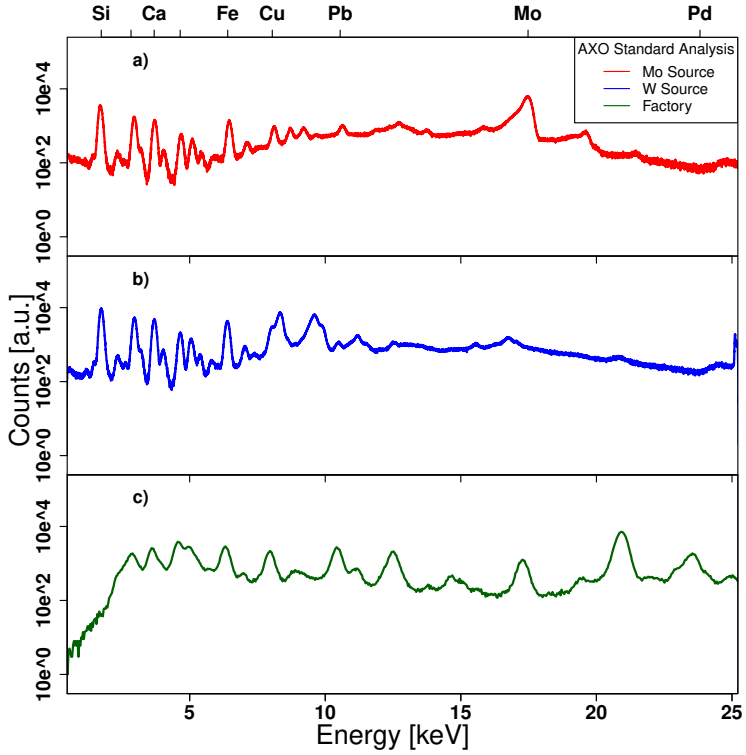

Figure 3. TXRF standard spectra from AXO. Red and blue data are obtained with our TXRF experimental setup, changing only the source anode ((**a**)—MoKα and (**b**)—W Bremsstrahlung respectively), while green (**c**) is the AXO data obtained with synchrotron radiation. Ruling out the elastic and inelastic peaks due to the source, our spectra are in good agreement with AXO data.

3.1. Environmental Analysis

Several natural archives may provide unaltered records of environmental and climatic information at different time scales dating back up to several hundred thousand years: marine sediments [31,32], stalagmite conformations [33], tree rings [13] and deep ice cores [14–16]. The analysis of tree rings is a powerful historical ecology tool because in tree species, inter- and intra-annual responses of radial growth to local climatic variations have been successfully assessed through the study of correlation and response functions among tree rings and monthly/weekly climatic factors. Moreover, dendrochemical analyses have shown the possibility of detecting the time accumulation of contaminants and pollutants in wood samples [13,34]. Measuring the chemical components concentrations in tree rings has powerful implications both for biological and ecological studies. Information on the spatial/temporal distribution within woody tissues of chemical elements such Ti, Ca and K, which represent basic cellular components or nutrients involved in basic physiological cellular processes, can provide key insights on how trees allocate nutrients in their tissues, e.g., according to species, the age, or other different environmental contexts. In addition, the capability of trees to store in their annual rings both inorganic (e.g., lead) and organic (e.g., HCH) pollutants can provide an a posteriori monitoring tool to quantitatively reconstruct the time dynamics of pollution over a territory [13,17].

In order to identify a preparation procedure for 2D μXRF mapping analysis for the entire core or for a slice about 500 μm thick, we prepared and tested a set of samples from different species, both conifers and angiosperms (figure in Supplementary Materials).

The results point out that together with the expected Ca, Ti and K, we have recorded the presence of high Z elements such as Cr, Fe and Zn. In Figure 4, we show a partial 2D μXRF mapping. The experimental parameters were 100×100 μm^2 steps with 10 s/step acquisition time. The colors (red and blue) representing Ca and Ti and their occurrence in tree rings perfectly reproduced the

sequence of different bands of earlywood and latewood, allowing one to position the different elements present as inclusions on a temporal scale.

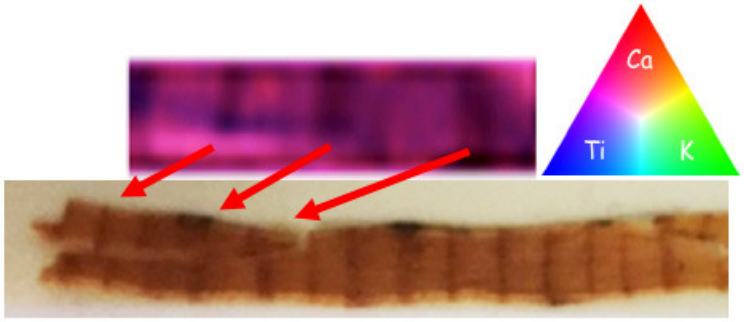

Figure 4. Section of the 2D mapping μXRF. Both Ca (red) and Ti (blue) reproduce the the time sequence of tree rings.

Deep ice cores can provide unaltered records of environmental and climatic changes at different time scales. Moreover, the mineralogical composition as well as the size distribution of particles are related to the dust transport in the atmosphere. Because of this, the dust deposed in the ice cores may provide a record of annual temperature, precipitation, atmospheric composition, volcanic activity and winds [16].

In collaboration with the University of Milan Bicocca and Diamond Lightsources, several samples have been analyzed at XlabF. Antarctic samples previously examined using synchrotron radiation at the Diamond Lightsource and the Stanford Synchrotron Radiation Lightsource (SSRL) have been analyzed, in order to compare the results and to evaluate the mass resolution of our prototype for elemental analysis of low concentration samples [6,7].

As a comparison, in Figure 5, two sets of XRF analysis are reported and compared. For the first set, a sample was deposited on a nuclepore membrane to be analyzed at normal incidence (XRF). For comparison, we reported also the same sample obtained by insoluble dust from Alps ice core (Saharian), analyzed with our prototype and with synchrotron radiation (Diamond Lightsource B-18). Despite the lower intensity on the fluorescence peaks and the higher noise, all elements of interest can also be recognized with our system.

The second example concerns TXRF spectra of a sample of insoluble dust from an Antarctic ice core collected with our prototype and with synchrotron radiation (SSRL Beamline BL-10.2). For both spectra, the measurement conditions were the same: vacuum $\sim 10^{-4}$ hPa for an acquisition time of 600 s. Due to the particular geometry of our system, the detector has to be placed at the Bragg angle ($\sim 40^{\circ}$) of the Si (400) of the sample and for this reason the silicon diffraction peak (DP) is measured at 7.5 keV. The prototype is able to recognize all the elements of interest in spite of the lower intensity and higher S/N ratio. An upper limit of 10 ng was identified for the interested elements (upper continental crust elements—UCC): Mg, Al, Si, S, Cl, K, Ca, Ti, Mn and Fe. The use of polycapillary semi-lens greatly improves the detection limits of TXRF with a standard source. Although the results remain below that available using an SR source, such a prototype can be used to perform many TXRF researches.

As a summary, Figure 6-top shows the concentrations for both layouts. Using the TXRF layout, the concentration detection is comparable with a synchrotron radiation source, while using the XRF layout our prototype is substantially not comparable with the detection capability of SR, even if samples from the Alps have about one order of magnitude higher concentration with respect to the Antarctic ones. Accordingly, for XRF measurements, our prototype is not suitable for extremely low concentrated samples, such as those from Antarctica. Figure 6-bottom shows the signal-to-noise ratio (SNR) in order to evaluate the limit of detection (LOD), analyzing only the elements in the UCC list. It is important to remark that these LODs are not absolute values, but they are calculated peak to peak for these samples and in a different experimental setup. For TXRF, silicon's SNR is affected by an intrinsic error.

The beam coming from a polyCO semi-lens has millimetric dimensions, so a fraction of the beam contacts the Si-wafer directly.

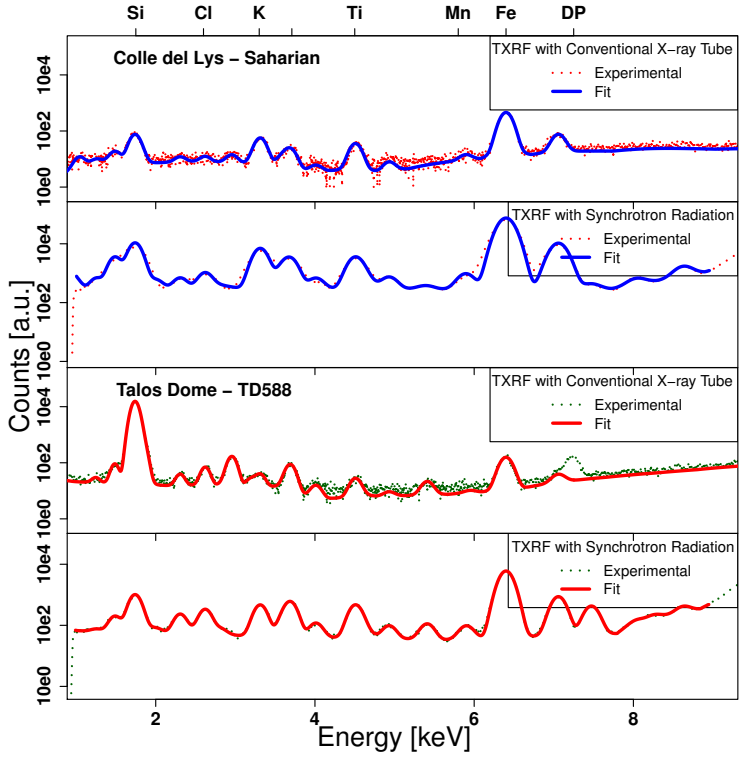

Figure 5. TXRF comparison between our desktop and the Synchrotron Radiation (SR) setup for XRF (first set—Alps sample) and for TXRF (second set—Antarctica sample) measurements.

As a summary, in the top panel of Figure 6, we show the concentrations for both layouts. Using the TXRF layout, the concentration detection is comparable to a synchrotron radiation source, while using the XRF layout the prototype does not compare with the high detection capability of SR. This holds even for Alpine samples with about a one order of magnitude higher concentration with respect to the Antarctic ones. Accordingly, for XRF measurements, this prototype is not suitable for extremely low concentrated samples, such as those from Antarctica. In the bottom panel of Figure 6, to evaluate the limit of detection (LOD) we show the signal-to-noise ratio (SNR) of the elements of the UCC list. It is important to remark here that LODs are not absolute values, but they are values calculated peak to peak for these samples and with this experimental setup. For TXRF, silicon's SNR is affected by an intrinsic error: the beam coming from a polyCO semi-lens has millimeter size dimensions and a fraction of the beam contacts the Si wafer directly. In our sample, magnesium is under the LOD limit, because its energy is near the lower electronic limit of the detector (∼1 keV) and because of the very low concentration—about 2–3% of the sample weight.

For samples from deep ice cores, the preparation technique for XRF measurements is the filtration. The latter presents during the deposition on the membrane some drawbacks such as the coffee stain. Moreover, one of the critical issues is the low superficial density of the deposited dust, highlighted in Figure 6 by the low efficiency of XRF analysis working at normal incidence than synchrotron radiation data. To increase the sample density and the homogeneity of the deposition, new deposition methods based on the micro-drop technique are under test [35]. At present, all samples prepared for TXRF analysis were deposited on Si wafers. However, since the silicon is the element present with the highest concentration in environmental and geological samples, the quantitative analysis of Si with this technique is overestimated. To overcome this issue, other substrates such as lithium fluoride (LiF) crystals are also under test. These preparation methods may certainly enhance the capability of

prototypes based on conventional sources with optimized optics if the contaminants present in these substrates are as low as in silicon wafer.

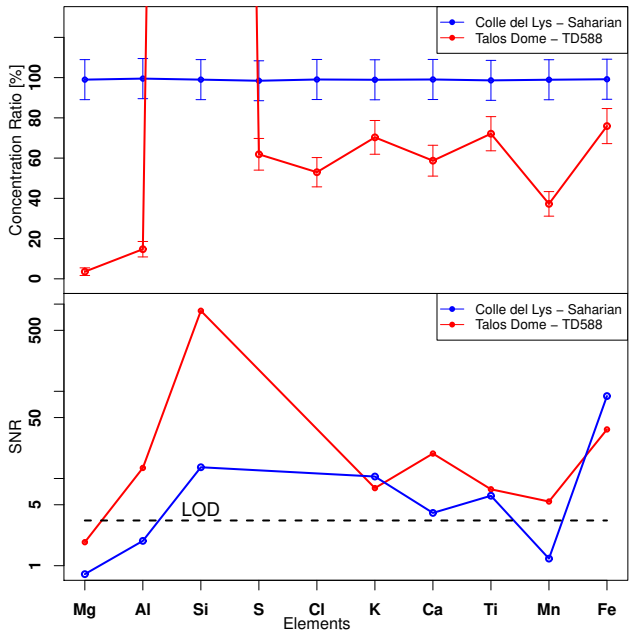

Figure 6. (**Top**) Concentration ratio for the samples in Figure 5. In the TXRF layout, a comparable concentration detection is achieved, while for the XRF modality the elements concentrations are not comparable. (**Bottom**) The signal-to-noise ratio (SNR) is analyzed in order to evaluate the limit of detection (LOD) of our system with these samples. The elements analyzed are the only in the upper continental crust elements (UCC) list. The Si element has an intrinsic error: the beam coming from a polyCO semi-lens has millimetric dimensions. Thus, a fraction of the beam directly contacts the Si wafer.

4. Conclusions

The peculiar capability of polycapillary optics to obtain a powerful quasi-parallel beam from a divergent source provides great opportunities for elemental analysis by using both XRF and TXRF even for very low concentration samples. The comparison with synchrotron radiation data shows that the results presented in this contribution are particularly interesting. Indeed, data of two independent sets show good agreement with experimental data collected using SR. The agreement is particularly good at energies up to the Fe K-emission line, indicating that a conventional X-ray source combined with polycapillary optics is a valuable alternative for many analysis in samples with elemental concentrations down to ng/g. Best results were obtained with the TXRF layout. However, this technique requires a sample preparation to be optimized for geological researches, particularly regarding the substrate and the sample deposition method. Currently, we are evaluating two different types of substrates such as LiF crystals and polymeric films. However, the final choice must be to pay particular attention to the presence of contaminants in the substrates. Work is also in progress to optimize the deposition method and in particular to increase the sample density and the deposition homogeneity.

Supplementary Materials: Supplementary Materials can be found at: http://www.mdpi.com/2410-3896/3/4/33/s1.

Author Contributions: D.H., S.B.D., G.C. and A.M. are responsible of the project and realization of the RXR experimental setup and development of the control software, V.M is the team leader of the Antarctic and Alps drilling sites, A.d.F. and G.P. provided the tree samples. All authors have read and approved the final manuscript.

Funding: This research received no external funding.

Acknowledgments: One of the authors (S.B.D.) acknowledges the support by the Competitiveness Program of NRNU MEPhI. In collaboration with the Laboratory of Dendroecology of the Department of Agriculture and Forest Science (DAFNE) of the University of Tuscia, we started at XlabF to develop a protocol to analyze tree-ring cores necessary to monitor beech forests patronaged by UNESCO. In collaboration with the University of Milan Bicocca and Diamond Lightsources, several samples have been analyzed using synchrotron radiation at the Diamond Lightsource and the Stanford Synchrotron Radiation Lightsource (SSRL).

Conflicts of Interest: The authors declare no conflict of interest.

Abbreviations

The following abbreviations are used in this manuscript:

PolyCO	Polycapillary Optics
XRF	X-ray Fluorescence
μXRF	micro X-ray Fluorescence
TXRF	Total Reflection X-ray Fluorescence
SR	Synchrotron Radiation
UCC	Upper Continental Crust

References

1. Tsuji, k.; Nakano, K.; Hayashi, H.; Hayashi, K.; Ro, C. X-ray Spectrometry. *Anal. Chem.* **2008,** 80, 4421–4454. [CrossRef] [PubMed]
2. Hampai, D.; Dabagov, S.B.; Cappuccio, G.; Longoni, A.; Frizzi, T.; Cibin, G.; Guglielmotti, V.; Sala, M. Elemental Mapping and Micro-Imaging by X-Ray Capillary Optics. *Opt. Lett.* **2008,** *33,* 2743–2745. [CrossRef] [PubMed]
3. Giannoncelli, A. In Proceedings of the 24th International Congress on X-Ray Optics and Microanalysis, Trieste, Italy, 25–29 September 2017.
4. Croudace, I.W.; Rothwell, R.G. *MIcro-XRF Studies of Sediment Cores*; Springer: Berlin, Germany, 2015.
5. Shackley, M.S. *X-ray Fluorescence Spectrometry (XRF) in Geoarchaeology*; Spinger: Berlin, Germany, 2011.
6. Cibin, G.; Marcelli, A.; Maggi, V.; Sala, M.; Marino, F.; Delmonte, B.; Albani, S.; Pignotti, S. First combined total reflection X-ray fluorescence and grazing incidence X-ray absorption spectroscopy characterization of aeolian dust archived in Antarctica and Alpine deep ice cores. *Spectrochim. Acta B* **2008**, *63,* 1503–1510. [CrossRef]
7. Marcelli, A.; Cibin, G.; Hampai, D.; Giannone, F.; Sala, M.; Pignotti, S.; Maggi, V.; Marino, F. XANES characterization of deep ice core insoluble dust in the ppb range. *J. Anal. At. Spectrom.* **2012**, *22*, 33–37. [CrossRef]
8. Dabagov, S.B. Channeling of neutral particles in micro- and nanocapillaries. *Phys. Uspekhi* **2003**, *46,* 1053–1075. [CrossRef]
9. Hampai, D.; Cherepennikov, Y.M.; Liedl, A.; Cappuccio, G.; Capitolo, E.; Iannarelli, M.; Azzutti, C.; Gladkikh, Y.P.; Marcelli, A.; Dabagov, S.B. Polycapillary based μXRF station for 3D colour tomography. *JINST* **2018**, *13,* C04024. [CrossRef]
10. Hampai, D.; Liedl, A.; Cappuccio, G.; Capitolo, E.; Iannarelli, M.; Massussi, M.; Tucci, S.; Sardella, R.; Sciancalepore, A.; Polese, C.; et al. 2D-3D μXRF elemental mapping of archeological samples. *Nucl. Instrum. Methods B* **2017**, *402,* 274–277. [CrossRef]
11. Zoeger, N.; Streli, C.; Wobrauschek, P.; Jokubonis, C.; Pepponi, G.; Roschger, P.; Hofstaetter, J.; Berzlanovich, A.; Wegrzynek, D.; Chinea-Cano, E.; et al. Determination of the elemental distribution in human joint bones by SR micro XRF. *X-Ray Spectrom.* **2008**, *37,* 3–11. [CrossRef]
12. Nakano, K.; Tanaka, K.; Ding, X.; Tsuji, K. Development of a new total reflection X-ray fluorescence instrument using polycapillary X-ray lens. *Spectrochim. Acta B* **2006**, *61,* 1105–1109. [CrossRef]
13. Bernini, R.; Pelosi, C.; Carastro, I.; Venanzi, R.; Di Filippo, A.; Piovesan, G.; Ronchi, B.; Danieli, P.P. Dendrochemical investigation on hexachlorocyclohexane isomers (HCHs) in poplars by an integrated study of micro-Fourier transform infrared spectroscopy and gas chromatography. *Trees Struct. Funct.* **2016**, *30,* 1455–1463. [CrossRef]

14. Petit, J.R.; Jouzel, J.; Raynaud, R.; Barkov, N.I.; Barnola, J.M.; Basile, I.; Bender, M.; Chappellaz, J.; Davis, M.; Delaygue, G.; et al. Climate and atmospheric history of the past 420,000 years from the Vostok ice core, Antarctica. *Nature* **1999**, *399*, 429–436. [CrossRef]
15. Community Members EPICA. Eight glacial cycles from an Antarctic ice core. *Nature* **2004**, *429*, 623–628. [CrossRef] [PubMed]
16. Maggi, V. Mineralogy of atmospheric microparticles deposited along the Greenland Ice Core Project ice core. *J. Geophys. Res.* **1997**, *102*, 26725–26734. [CrossRef]
17. Sawidis, T.; Breuste, T.; Mitrovic, M.; Pavlovic, P.; Tsigaridas, K. Trees as bioindicator of heavy metal pollution in three European cities. *Environ. Pollut.* **2011**, *159*, 3560–3570. [CrossRef] [PubMed]
18. Hampai, D.; Dabagov, S.B.; Cappuccio, G. Advanced studies on the Polycapillary Optics use at XLab Frascati. *Nucl. Instrum. Methods B* **2015**, *355*, 264–267. [CrossRef]
19. Nanoray, a portable X-ray machine. FP7 Project N 222426 (2008-2011). Available online: https://www.parlementairemonitor.nl/9353000/1/j9tvgajcor7dxyk_j9vvij5epmj1ey0/vj4871mm6efo?ctx=vg9pjpw5wsz1&start_tab0=1160 (accessed on 18 October 2018).
20. Hampai, D.; Dabagov, S.B.; Cappuccio, G.; Cibin, G.; Sessa, V. X-ray micro-imaging by capillary optics. *Spectrochim. Acta Part B* **2009**, *64*, 1180–1184. [CrossRef]
21. Cherepennikov, Y.; Miloichikova, I.; Gogolev, A.; Stuchebrov, S.; Hampai, D.; Dabagov, S.; Liedl, A. Application of polycapillary optics for dual energy spectroscopy based on a laboratory source. *Nucl. Instrum. Methods B* **2017**, *402*, 278–281. [CrossRef]
22. Liedl, A.; Dabagov, S.B.; Hampai, D.; Polese, C.; Tsuji, K. On X-ray channeling in a vibrating capillary. *Nucl. Instrum. Methods B* **2015**, *355*, 289–292. [CrossRef]
23. Marchitto, L.; Hampai, D.; Dabagov, S.B.; Allocca, L.; Alfuso, S.; Polese, C.; Liedl, A. GDI spray structure analysis by polycapillary X-ray μ-tomography. *Int. J. Multiph. Flow* **2015**, *70*, 15–21. [CrossRef]
24. Bonfigli, F.; Hampai, D.; Dabagov, S.B.; Montereali, R.M. Characterization of X-ray polycapillary optics by LiF crystal radiation detectors through confocal fluorescence microscopy. *Opt. Mater.* **2016**, *58*, 398–405. [CrossRef]
25. Gogolev, A.S.; Hampai, D.; Khusainov, A.K.; Zhukov, M.P.; Dabagov, S.B.; Potylitsyn, A.P.; Liedl, A.; Polese, C. Results of testing the energy dispersive Si detector with large working area. *Nucl. Instrum. Methods B* **2015**, *355*, 268–271. [CrossRef]
26. Available online: http://www.oxford-instruments.com (accessed on 18 October 2018).
27. Available online: http://www.xglab.it (accessed on 18 October 2018).
28. Available online: http://www.photonic-science.com (accessed on 18 October 2018).
29. Available online: https://www.physikinstrumente.com/en/ (accessed on 18 October 2018).
30. Available online: http://www.axo-dresden.de/products/highprecision/reference.htm (accessed on 18 October 2018).
31. Bostick, B.C.; Theissen, K.M.; Dunbar, R.B.; Vairavamurthy, A. Record of redox status in laminated sediments from Lake Titicaca: A sulfur K-edge X-ray absorption near edge structure (XANES) study. *Chem. Geol.* **2005**, *219*, 163–174. [CrossRef]
32. Moy, C.M.; Dunbar, R.B.; Guilderson, T.P.; Waldmann, N.; Mucciarone, D.A.; Recasens, C.; Ariztegui, D.; Austin, J.A., Jr.; Anselmetti, F.S. A geochemical and sedimentary record of high southern latitude Holocene climate evolution from Lago Fagnano, Tierra del Fuego. *Earth Planet. Sci. Lett.* **2011**, *302*, 1–13. [CrossRef]
33. Polyak, V.J.; Asmerom, Y. Late Holocene Climate and Cultural Changes in the Southwestern United States. *Science* **2001**, *294*, 148–151. [CrossRef] [PubMed]
34. Di Filippo, A.; Biondi, F.; Cûfar, K.; De Luis, M.; Grabner, M.; Maugeri, M.; Presutti Saba, E.; Schirone, B.; Piovesan, G. Bioclimatology of beech (*Fagus sylvatica* L.) in the Eastern Alps: Spatial and altitudinal climatic signals identified through a tree-ring network. *J. Biogeogr.* **2007**, *34*, 1873–1892. [CrossRef]
35. Macis, S.; Cibin, G.; Maggi, V.; Baccolo, G.; Hampai, D.; Delmonte, B.; D'Elia, A.; Marcelli, A. Microdrop Deposition Technique: Preparation and Characterization of Diluted Suspended Particulate Samples. *Condens. Matter* **2018**, *3*, 21. [CrossRef]